Journal of Fluorescence (2022) 32:1651–1660
https://doi.org/10.1007/s10895-022-02961-y

ORIGINAL ARTICLE

Fluorescent Biosensor Based on Hairpin DNA Stabilized Copper Nanoclusters for *Chlamydia trachomatis* Detection

Luyao Liu[1,2,3] · Qinqin Bai[1,2,3] · Xuebing Zhang[1,2,3] · Chunxue Lu[4] · Zhongyu Li[4] · Hao Liang[1,2,3] · Lili Chen[1,2,3]

Received: 10 January 2022 / Accepted: 20 April 2022 / Published online: 25 May 2022

Abstract

Chlamydia trachomatis (C. trachomatis) is a kind of intracellular parasitic microorganism, which can causes many diseases such as trachoma. In this strategy, a specific hairpin DNA with the probe loop as specific regions to recognize *C. trachomatis* DNA with strong affinity was designed, and its stem consisted of 24 AT base pairs as an effective template for hairpin DNA-CuNCs formation. In the absence of *C. trachomatis* DNA, the detection system showed strong orange fluorescence emission peaks at 606 nm. In the presence of *C. trachomatis* DNA, the conformation of DNA probe changed after hybridizing with *C. trachomatis* DNA. Then, the amount of hairpin DNA-CuNCs was reduced and resulted in low fluorescence emission. *C. trachomatis* DNA displayed a significant inhibitory effect on the synthesis of fluorescent hairpin DNA-CuNCs due to the competition between *C. trachomatis* DNA and the specific hairpin DNA. Under the optimal experimental conditions, different concentrations of *C. trachomatis* were tested and the results showed a good linear relationship in the range of 50 nM to 950 nM. Moreover, the detection limit was 18.5 nM and this detection method possessed good selectivity. Finally, the fluorescent biosensor had been successfully applied to the detection of *C. trachomatis* target sequence in HeLa cell lysate, providing a new strategy for the detection of *C. trachomatis*.

Keywords *Chlamydia trachomatis* · CuNCs · Detection · Hairpin DNA

Introduction

Chlamydia trachomatis (*C. trachomatis*) is an obligate intracellular parasite and a prokaryotic cell-type microorganism with a unique development cycle that can cause a variety of diseases in humans and animals, such as trachoma, urethral syndrome, venereal lymphogranuloma, male urethritis, epididymitis, cervicitis, pelvic inflammatory disease [1–3]. In the early stage of *C. trachomatis* infection, the immune response of most patients is mainly the neutralization of IgA, which limits the spread of inflammation but cannot completely eliminate *C. trachomatis*. Therefore, the patient has no obvious clinical symptoms during this period, which often leads to occult infection and chronic persistent infection. With the continuous survival and reproduction of *C. trachomatis* in host cells, the Arthus response (a type of local type III hypersensitivity reaction) is initiated, and the immune complexes produced can cause epithelial cell damage and fibrosis and scarring of infected organs. The diseases caused by *C. trachomatis* develop gradually and imperceptibly that can affect multiple organs and bring serious consequences. Therefore, rapid diagnosis of *C. trachomatis* infection is of great significance for early clinical diagnosis and guided treatment.

Conventional methods for clinical detection of *C. trachomatis* include isolation and cell culture [4], serological diagnostic methods [5, 6], and PCR-based nucleic acid amplification technologies [7, 8]. Although the classical

✉ Hao Liang
8483064@qq.com

✉ Lili Chen
chlili720612@163.com

1 Department of Public Health Laboratory Sciences, School of Public Health, Hengyang Medical School, University of South China, Hengyang 421001, Hunan, China

2 Hunan Key Laboratory of Typical Environmental Pollution and Health Hazards, School of Public Health, Hengyang Medical School, University of South China, Hengyang 421001, Hunan, China

3 Hengyang Engineering Technology Research Center, Hengyang 421001, Hunan, China

4 Institute of Pathogenic Biology, Hengyang Medical School, University of South China, Hengyang 421001, Hunan, China

isolation and culture methods are specific, they are time-consuming and not sensitive enough to be suitable for rapid clinical detection; It is generally believed that serological diagnostic methods are of little significance in the diagnosis of *C. trachomatis* infection because of their's powerlessness of make a diagnosis in the early stages of microbial infection and distinguish between previous infections and new infections; PCR and other molecular biological methods are prone to false positive and have high requirements on the instrument, which limits their applications in the primary laboratory. Therefore, the development of a simple, rapid and highly sensitive biosensor for the detection of *C. trachomatis* is of great significance for disease diagnosis and public health.

The major outer membrane protein (MOMP) of *C. trachomatis* is an intrinsic component of its outer membrane, which is recognized as the major epitope and present in all serotypes [9]. MOMP is mainly composed of single copy gene *omp1*, which contains 5 stable sequence regions and 4 variable sequence regions spaced apart. The sequence of the 5 stable sequence regions is very conservative, and the differences between different serotypes are very small [10]. Nucleic acid hybridization detection of specific DNA or RNA sequences of *C. trachomatis* has significantly better sensitivity and specificity than the detection of protein based on antigen–antibody immune response [11, 12]. Consequently, the conserved sequence of the *omp1* gene of *C. trachomatis* can be utilized as the target sequences for *C. trachomatis* detection.

Copper nanoclusters (CuNCs) are relatively stable aggregates composed of several to several hundred copper atoms through physical and chemical binding forces, with particle size generally less than 3 nm. Compared with other precious metal elements such as gold and silver, the reserves of cuprum are more abundant in nature and lower cost, making the application prospect of CuNCs broader [13]. The effective templates for the synthesis of CuNCs are generally double-stranded DNA (dsDNA) or single-stranded polythymine (poly(T)) DNA [14]. Furthermore, it has been reported that CuNCs with better fluorescence performance could be synthesized by hairpin DNA [15, 16]. Zhang et al. developed a low-cost and enzyme-free method for detecting microcystins using hairpin DNA templated CuNCs as fluorescent probes based on the specific affinity of microcystins and their aptamers, and the detection limit was 0.003 ng/L [17]. Wu et al. used CuNCs as fluorescent signals to achieve clinical classification of genes for duchenne muscular dystrophy [18]. Different types of exons of duchenne muscular dystrophy genes as model analytes for genetic diagnosis were amplified by polymerase chain reaction (PCR), and then utilized to be the templates for synthesizing CuNCs and generated fluorescent signals of different intensities correspondingly. This method was successfully applied to the clinical examination of patients, and the actual samples were consistent with the clinical diagnosis results.

In this study, we designed a specific hairpin DNA for *C. trachomatis* detection. The stem of the hairpin DNA had 24 pairs of AT bases as a template for CuNCs, and 35 base probe loop served as a specific region for recognizing the target DNA of *C. trachomatis*. In the present of target DNA, the hairpin DNA was opened with the changing of the template for synthesis of CuNCs, resulting in the fluorescence intensity of CuNCs significantly decreased. Based on this strategy, a simple, rapid and highly sensitive fluorescent biosensor for *C. trachomatis* detection was achieved, which is of great significance for the early diagnosis and treatment of infectious diseases.

Experimental

Reagent and Apparatus

The 3-(N-morpholino)-propanesulfonic acid (MOPS) was obtained from Sangon Biotech Co., Ltd (Shanghai, China). Copper sulfate pentahydrate ($CuSO_4 \bullet 5H_2O$) was purchased from Hunan Huihong Reagent Co., Ltd (Changsha, China). Ascorbic acid (AA) and sodium ascorbate (SA) were provided from Macklin Biochemical Technology Co., Ltd (Shanghai, China). Sodium borodeuteride ($NaBH_4$) and hydrazine monohydrate ($N_2H_2 \bullet H_2O$) were purchased from Sinopharm Chemical Reagent Co., Ltd (Shanghai, China). All reagents were prepared by dissolving with ultra pure water with resistance > 18.3MΩ except nucleic acid solution. All the oligonucleotides used in this study were synthesized by Sangon Biotech Co., Ltd (Shanghai, China) and purified with HPLC. All nucleic acid solutions were prepared using sterile DEPC water before use.

Specific probes were designed in accordance with the conserved region of *omp1* gene of *C. trachomatis* by the software of oligo7.0. The following oligonucleotide sequences were synthesized by Shanghai Sangon Biotechnology Co., Ltd and purified by HPLC. The specific sequences are as follows:

Probe AT24 hairpin sequence (the underlined was the target *omp1* gene sequence): 5′-ATA TAT ATA TAT ATA TAT ATA TAT <u>GCC GAG ACT ATC TTT GAT GTT ACC ACT CTG AAC CC</u>A TAT ATA TAT ATA TAT ATA TAT AT -3′;

C. trachomatis (CT): 5′-GGG TTC AGA GTG GTA ACA TCA AAG ATA GTC TCG GC -3′:

HPV: 5′-GTTCT GCTCC ATCTG CCACT ACGTC TTCTA AACCT-3′;

HSV-2: 5′-ACTCC GATTC GACCA CATAT GCAAC CAAAT CACCC-3′;
Lactobacillus: 5′-ACAGT TACAA TGAAG GCGAA AAGAA GGTTG ATAAT-3′;
Candida albicans: 5′-GTTTG CTTGA AAGAC GGTAG TGGTA AGGCG GGATC-3′;
Treponema pallidum: 5′-CATCA TCAGG AAGGA AAAGA CATCG CAGCG CTTAC-3′;
Neisseria gonorrhoeae: 5′-GATAT CTGAT TAGCT AGTTG GTGGG GTAAA GGCCT-3′;
Ureaplasma urealyticum: 5′-TTATT GATTT AGTCG GAACA CGTTG AAGTT TGAGG-3′.

Apparatus

Ultraviolet absorption spectrum data were collected with UV-2550 UV–visible spectrophotometer (Shimadzu Instruments, Japan). The scanning wavelength range of UV–visible spectrum was set at 200 ~ 700 nm, and ultra-pure water were used as blank reference solution, baseline scanning and background deduction zeroing were performed before detection. Fluorescence spectra data were collected with Lumina fluorescence spectrophotometer (Thermo Fisher Scientific, USA) equipped with a Xenon lamp excitation source, slit widths for the excitation and emission were both set at 10 nm, and the PMT voltage was set to 700 V. The fluorescence emission spectra from 450 to 680 nm were collected at room temperature at 345 nm excitation wavelength. Visual and fluorescence emission photographs were acquired under 365 nm three-way ultraviolet analyzer instrument (ZF-2, Shanghai, China) by smartphone. Transmission electron microscopy (TEM) results were obtained using a Tecnai G2 F20 S-TWIN microscope (FEI, USA). Ultrapure water is produced by ELGA Purification Facility (USF ELGA, Germany). pH values of all solutions were measured using a PB-10 pH meter (Sartorius, Germany).

Synthesis of Fluorescent Hairpin DNA-CuNCs

Hairpin DNA-CuNCs were prepared according to the classic AA reduction method: First, a certain concentration of hairpin DNA solution was annealed in an annealing buffer at 95 °C for 5 min, and then slowly cooled to room temperature (25 °C) to form a hairpin secondary structure. Then, AA solution was added to the above solution, 1 min later, $CuSO_4$ solution was added into the mixture solution. Finally, the MOPS buffer (10 mM MOPS, 150 mM NaCl, pH 7.5) was added to the above solution to make up to a final volume of 100 μL. The mixture solution was incubated in a 25 °C for 15 min in the dark to obtain the fluorescent hairpin DNA-CuNCs, then stored at 4 °C in the dark.

Agarose Gel Eletrophoresis

DNA templates, annealing products and synthetic products were characterized by 3% agarose gel electrophoresis. Different DNA samples were obtained by adding reactions in different swimming lanes. The electrical pressure was set at 70 V, and the samples were run in 1 × TAE electrophoresis buffer at chamber temperature, and the results were photographed under UV lamp.

Fluorescent Detection of C. Trachomatis

First, a certain concentration gradient target *omp1* gene of *C. trachomatis* and 5 μL hairpin DNA template (500 nM) nucleic acid solution were mixed in different ep tubes, respectively. Then, the mixed solution was placed in PCR instrument with an annealing gradient of 95 °C for 5 min, and then slowly cooled to room temperature (25 °C). Add 1 mM of freshly prepared AA solution in the above solution after processing, mixing the solution for 1 min, add $CuSO_4$ solution and MOPS buffer to a final volume of 100 μL. After thoroughly mixing and centrifugalization, the resulting solution was incubated for 5 min in the dark in an incubator at 25 °C. The samples without target *omp1* gene were taken as blank control, and theirs fluorescence intensity were determined as F_0. The fluorescence intensity detected by the samples with a certain concentration gradient was set as F. Record the fluorescence intensity of the system at 606 nm using a Lumina fluorescence spectrophotometer. To obtain the detection limit (LOD), the blank sample without *C. trachomatis* was measured 11 times repeatedly, and its relative standard deviation (RSD) was obtained as δ, and the LOD was calculated by dividing 3 times the standard deviation by the slope (κ) of the fitted curve. All of the measurements were performed three times.

Selectivity Investigation

The DNA sequences of other pathogenic microorganisms that also invade the reproductive tract and the normal microorganisms of the female reproductive tract were used as interferences to evaluate the specificity of this method. Under the best experimental conditions, the human papillomavirus (HPV), herpes simplex virus (HSV-2), *Lactobacillus*, *Candida albicans*, *Treponema pallidum*, *Neisseria gonorrhoeae*, *Ureaplasma urealyticum*, a mixture of the above interference sequences, *C. trachomatis omp1* gene sequence, and a mixture of the above interference sequence and *C. trachomatis omp1* gene sequence were chosen as the test objects for the experiment (The concentration of interference sequence in the detection system was 8 μM and

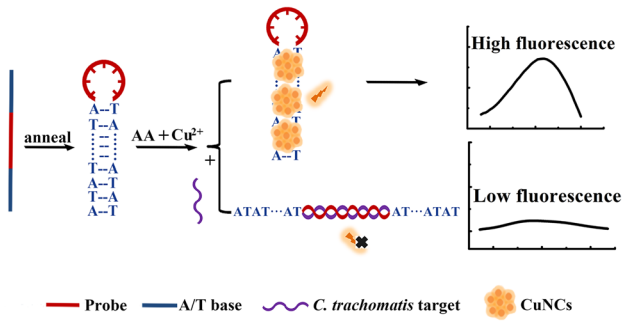

Fig. 1 Schematic diagram of fluorescent strategy for *C. trachomatis* detection based on hairpin DNA-CuNCs

C. trachomatis omp1 gene was 0.8 μM). The fluorescence intensity of each system was determined via Lumina fluorescence spectrophotometer.

Results and discussion

Hairpin DNA-CuNCs Sensing Strategy

The effective templates for synthesizing fluorescent CuNCs are double-stranded poly (AT) sequence and single-stranded poly (T) sequence. The schematic diagram of the designed fluorescent biosensor for *C. trachomatis* detection is shown in Fig. 1. The probe loop of hairpin DNA (red fragment) acts as specific regions to recognize the target DNA of *C. trachomatis* with strong affinity, and the 24 AT base pairs (blue fragment) complementary double strand stem of hairpin DNA serves as an effective template for CuNCs formation. The base complementary pairing of the *C. trachomatis* target *omp1* DNA between the hairpin DNA probe result in the opening of the hairpin DNA and a significant inhibitory effect on the synthesis of CuNCs. Owing to this phenomenon, the fluorescent signals from CuNCs decreased and showed a good linear relationship with the different concentrations of *C. trachomatis* target DNA. Based on this principle, a qualitative and quantitative detection method of *C. trachomatis* can be achieved.

Characterization of Hairpin DNA-CuNCs

The synthesized hairpin DNA-CuNCs were characterized by fluorescence spectrometry, UV–vis spectroscopy and TEM. The fluorescence (FL) spectra in Fig. 2 revealed that excitation (curve c) and emission (curve d) of hairpin DNA-CuNCs were at 345 and 606 nm (both excitation and emission slits were 10 nm), respectively. As shown in Fig. 2A, the hairpin DNA solution has a characteristic UV absorption peak of DNA at around 260 nm (curve a). The characteristic absorption peak (Fig. 2A, curve b) was similar to the fluorescence excitation spectrum (Fig. 2A, curve c) appeared in the recorded absorption spectrum. In the ultraviolet–visible (UV–Vis) absorption spectrum of hairpin DNA-CuNCs, there was no absorption band at 560 ~ 600 nm (arising from surface plasmon resonance of copper nanoparticles), which indicated that no large size copper nanoparticles were formed [19]. In the illustration of Fig. 2A, we can observed that the hairpin DNA-CuNCs emitted obvious orange fluorescence under a 365 nm excitation. It could be seen from TEM results (Fig. 2B) that the synthesized CuNCs were similar to a spherical distribution, had regular shapes, and good dispersion in aqueous solution. The inset was a high-resolution image when the scale was 2 nm, and a clear lattice structure could be observed. Analyzed by Digital Micrograph software, the average particle size of hairpin DNA-CuNCs was obtained to be 2.12 nm, and the lattice spacing was

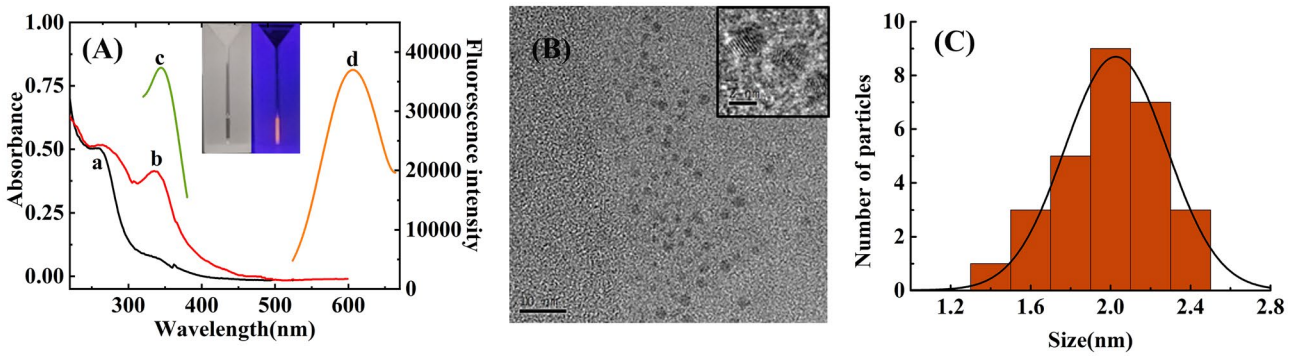

Fig. 2 Spectral and TEM characterization of hairpin DNA-CuNCs. (**A**) UV–Vis absorption and fluorescence spectra of hairpin DNA-CuNCs (UV absorption peaks of hairpin DNA probe (**a**) and hairpin DNA-CuNCs (**b**); Maximum fluorescence excitation peak (**c**) and maximum fluorescence emission peak (**d**) of hairpin DNA-CuNCs. Insert: Appearance of hairpin DNA-CuNCs under fluorescent lamp (left) and 365 nm ultraviolet lamp (right)); (**B**) The morphology of hairpin DNA-CuNCs under 10 nm TEM; (Insert: The morphology of hairpin DNA-CuNCs under 2 nm TEM); (**C**) The size distribution histogram of the hairpin DNA-CuNCs

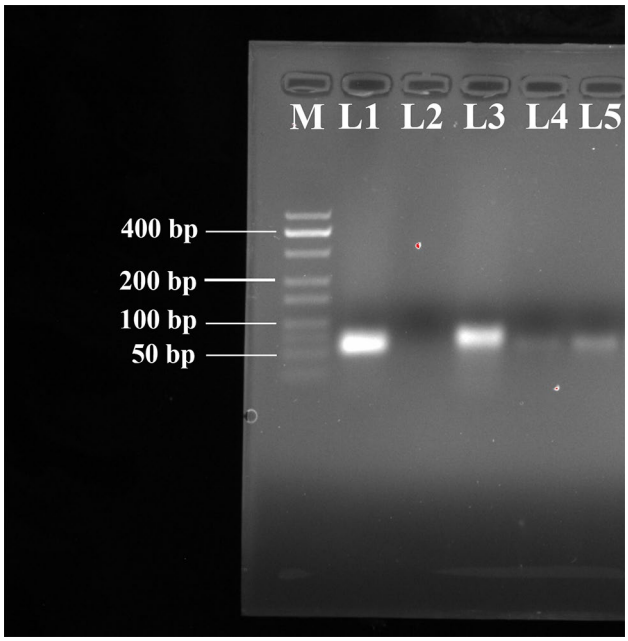

Fig. 3 Agarose gel electrophoresis diagrams of different reaction systems (3% gel concentration). M. DL500 DNA Marker; L1. AT24 hairpin probe; L2. *C. trachomatis omp1* gene; L3. AT24 hairpin probe + *C. trachomatis omp1* gene; L4. AT24 hairpin DNA-CuNCs; L5. AT24 hairpin DNA + *C. trachomatis omp1* gene-CuNCs

0.1989 nm. These results confirmed that the hairpin DNA-CuNCs were synthesized successfully and could provide strong fluorescence signals [20].

The Feasibility of the Fuorescent Biosensor for the C. Trachomatis Target Sequence Detection

In order to further support the above characterization results, we used 3% agarose gel electrophoresis to re-examine the feasibility of this method. A series of experimental groups were designed to verify the binding of the hairpin DNA probe to the target *omp1* DNA. The experimental results were shown in Fig. 3. Lane 1 (L1) was the band of hairpin DNA probe. Since the molecular weight of the target *omp1* DNA was too small, no band could be seen (Lane 2, L2). Lane 3 (L3) was the band of the hybridization product between the hairpin DNA probe and the target *omp1* sequence. Due to the larger weight than hairpin DNA probe, the band was lagging behind L1. Lane 4 (L4) was a band formed by CuNCs synthesized with hairpin DNA probe as template; Lane 5 (L5) was a band formed by CuNCs synthesized from the hybridization product between the hairpin DNA probe and the *C. trachomatis* target *omp1* sequence. The band was slightly lagging and brighter, again verifying the binding of the AT24 hairpin DNA probe to the *C. trachomatis* target *omp1* sequence. In summary, the verification result of electrophoresis was consistent with the aforementioned fluorescence characterization conclusion, which proved once more that our experimental principle and experimental program were indeed feasible.

Optimization of Experimental Conditions

The DNA template sequence had a decisive influence on the synthesis of CuNCs. According to the previous literature reports, poly (AT) dsDNA or poly T ssDNA were effective templates for generating fluorescent CuNCs [21, 22]. In this paper, the stem of the hairpin DNA was designed to be the template for the synthesis of fluorescent CuNCs. In order to realize the synthesis of CuNCs and the detection of *omp1* sequence at the same time, we designed five kinds of fluorescent probes, containing AT24 hairpin probe (AT24hp), ATT12 hairpin probe (ATT12 hp), T13 hairpin probe (T13 hp), T22 probe (T22), AT24 probe (AT24), to find the best hairpin probe for CuNCs synthesis. The specific sequence was shown in Table 1. The experimental results showed that the AT24 hairpin probe as template could provide the largest fluorescence (Fig. 4A).Therefore, the AT24 hairpin probe was chosen as the optimized sequence in subsequent experiments. Otherwise, Fig. 4B showed that the fluorescence intensity of haipin DNA-CuNCs gradually increased with the increase of the DNA template concentration (0.0, 0.1, 0.2, 0.3, 0.4, 0.5, 0.6 M) fluorescence intensity. When the concentration of AT24 hairpin probe was 0.5 M, the fluorescence intensity of the system reached the maximum. Therefore, 0.5 M was the optimized concentration of AT24 hairpin probe.

Table 1 Schematic diagram of the sequence and secondary structure of the label-free fluorescent probe

Name	Sequence (5'-3')
AT24 hairpin probe	ATATATATATATATATATATATATGCCGAGACTATCTTTGATGTTACCACTCTGAACCCATATATATATATATATATATATATAT
ATT12 hairpin probe	AATAATAATATAGCCGAGACTATCTTTGATGTTACCACTCTGAACCCATATTATTATT
T13 hairpin probe	GCATATCGTTTTTTTTTTTTTTCGATATGCGCCGAGACTATCTTTGATGTTACCACTCTGAACCC
T22 probe	TTTTTTTTTTTTTTTTTTTTTTGCCGAGACTATCTTTGATGTTACCACTCTGAACCC
AT24 probe	ATATATATATATATATATATATATGCCGAGACTATCTTTGATGTTACCACTCTGAACCC

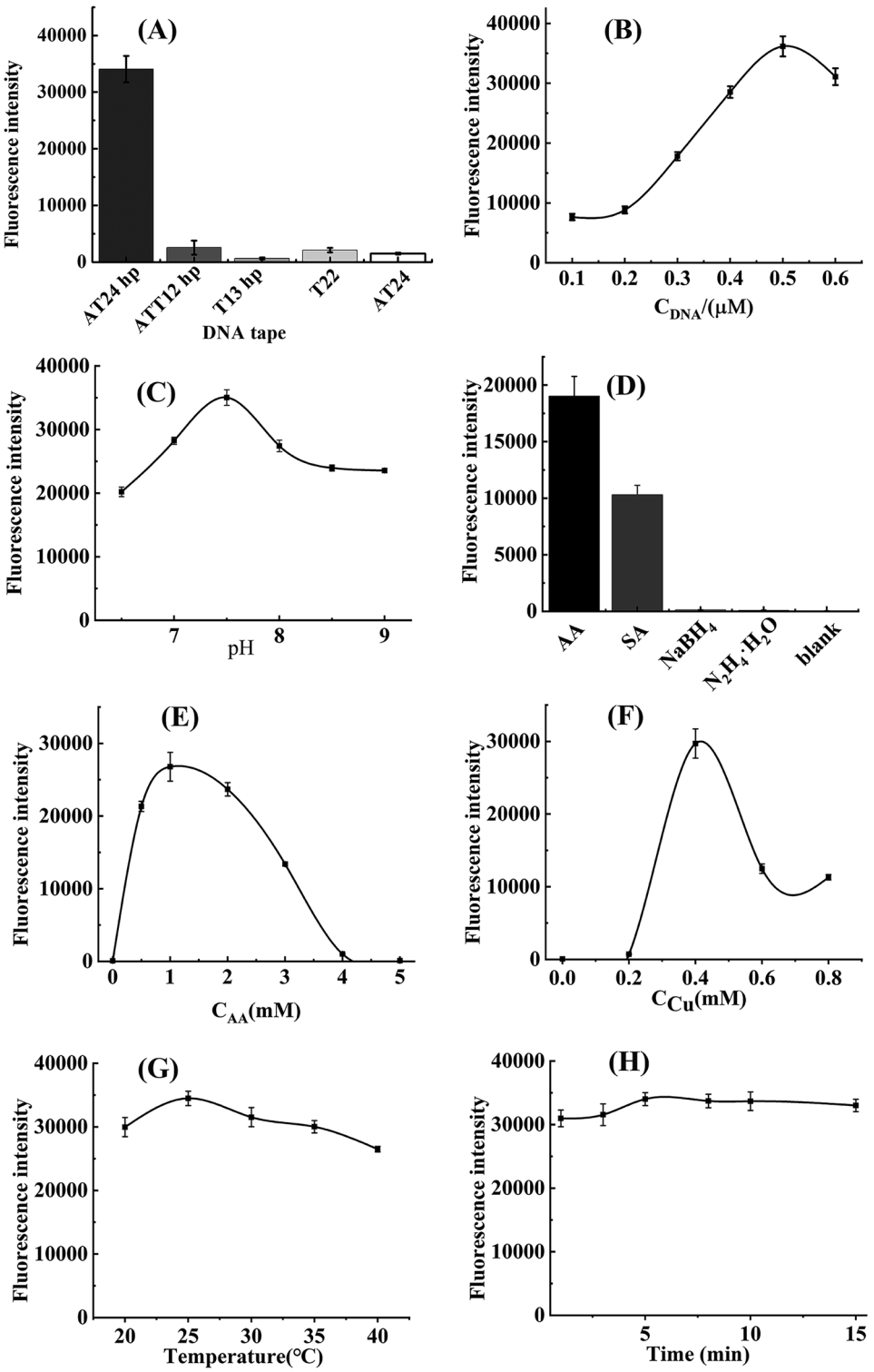

Fig. 4 Optimization of experimental conditions. (**A**) Optimization of DNA template type optimization. (**B**) DNA template concentration optimization. (**C**) Effect of buffer pH on the synthesis of CuNCs. (**D**) Reducing agent type optimization. (**E**) AA concentration optimization. (**F**) Optimization of Cu^{2+} concentration. (**F**) Optimization of the synthesis temperature of CuNCs. (**G**) Optimization of the synthesis time of CuNCs

In addition, to achieve an optimum detecting performance for detection of *C. trachomatis* target sequence, we investigated the effects of pH of buffer, type of reducing agent, concentrations of reducing agent and Cu^{2+}, and formation temperature and time of haipin DNA-CuNCs on the fluorescent intensity of haipin DNA-CuNCs probe.

The pH for haipin DNA-CuNCs synthesis had an important effect on the stability of CuNCs. The acidic buffer led to the rupture of hydrogen bonds of DNA double strand, further hydrolysis of phosphate diester bonds in the primary structure of DNA and the glycoside bonds inside nucleotides, which caused irreversible damage to DNA and decreased the

fluorescence intensity of CuNCs [23]. Therefore, the effect of MOPS buffer (pH 6.5 ~ 9.0) on the fluorescence intensity of the system was investigated. As depicted in Fig. 4C, the fluorescence intensity increased promptly with the pH value from 6.5 to 7.5. However, the fluorescence intensity started to drop when the pH value of MOPS buffer was higher than 7.5. Therefore, pH 7.5 was selected to ensure a good performance of our fluorescent biosensor.

The type and concentration of reducing agent was also an important parameter affecting the synthesis of CuNCs. As shown in Fig. 4D, at the same concentration of AA, SA, $NaBH_4$, $N_2H_2 \bullet H_2O$, and ultrapure water (blank), only the CuNCs synthesized with AA possessed the strongest fluorescence signal. And with the increase of AA concentration, the fluorescence intensity of CuNCs gradually increased. As a result, 1.0 mM AA was selected as the optimal reducing agent.

Cu^{2+} was reduced to Cu^0 and bound with DNA to form fluorescent CuNCs [24]. Low concentration of Cu^{2+} could not conducive to the synthesis of CuNCs. However, high concentrations of Cu^{2+} can react with AA to form a Fenton-like reaction to generate a lot of -OH free radicals. The -OH free radicals reacted with $-NH_2$ on the nucleic acid chain to break DNA strands and reduced the fluorescence intensity of CuNCs [25]. Therefore, the concentration of Cu^{2+} had an important effect on the fluorescence signal of CuNCs. As shown in Fig. 4F. the fluorescence intensity of CuNCs increased significantly with the increasing of Cu^{2+} concentration from 0.2 mM to 0.4 mM. As the concentration of Cu^{2+} increased by more than 0.4 mM, the fluorescence intensity started to decrease. Thus, 0.4 mM of Cu^{2+} solution was chosen as the optimal concentration for subsequent experiments.

Figure 4G have shown that CuNCs with higher fluorescence intensity could be synthesized at room temperature. When the temperature rised, the fluorescence signal had a downward trend. This might be due to the instability of the hairpin structure in high temperature, resulting in changes in the conformation of the template for CuNCs, thus affecting the synthesis of CuNCs and leading to lower fluorescence intensity. Accordingly, the optimized reaction temperature was 25 ℃.

The reaction time in the system was optimized. It could be seen from Fig. 4H that with the extension of the synthesis time of CuNCs, the fluorescence intensity of the system gradually increases with the increase of the reaction time, and reached the maximum at 5 min.

Analytical Performance of the Fluorescence Biosensor

The target DNA of *C. trachomatis* at different concentrations was detected under optimal experimental conditions. The results showed that the fluorescence intensity of the formed hairpin DNA-CuNCs gradually decreased with the increasing concentrations of *C. trachomatis* target DNA, the fluorescence intensity of CuNCs gradually decreased and F_0-F increased, where F and F_0 were the fluorescence intensities of the hairpin DNA-CuNCs in the presence and absence of the *C. trachomatis*, respectively. Figure 5B depicted the relationship between the *C. trachomatis* target DNA concentration and the fluorescence intensity of hairpin DNA-CuNCs at the maximum emission wavelength, showing a good linear correlation between the fluorescence intensity and the concentration of *C. trachomatis* target DNA in the range from 50 to 950 nM ($R^2 = 0.994$). This fitting linear equation could be expressed as $(F_0\text{-}F)/F_0 = 0.00115\boldsymbol{C}_{CT}(\text{nmol/L}) + 0.00574$. The LOD for *C. trachomatis* was calculated to be 18.5 nM (ignal-to-noise ratio of 3) based on 3δ/κ (δ was the standard deviation for the blank sample measurements without *C. trachomatis*, and κ was the slope of the fitting linear equation). The detection limit was estimated to be 18.5 nM, which was faster and more accurate than that of previously reported methods (Table 2), and the operation was simpler toward *C. trachomatis* target DNA detection. In addition, 11 tubes of *C. trachomatis* target sequence samples with low, medium and high concentrations (0.20, 0.40, 0.65 μM) were tested in parallel, and the RSD were 2.31%, 2.43% and 3.48%

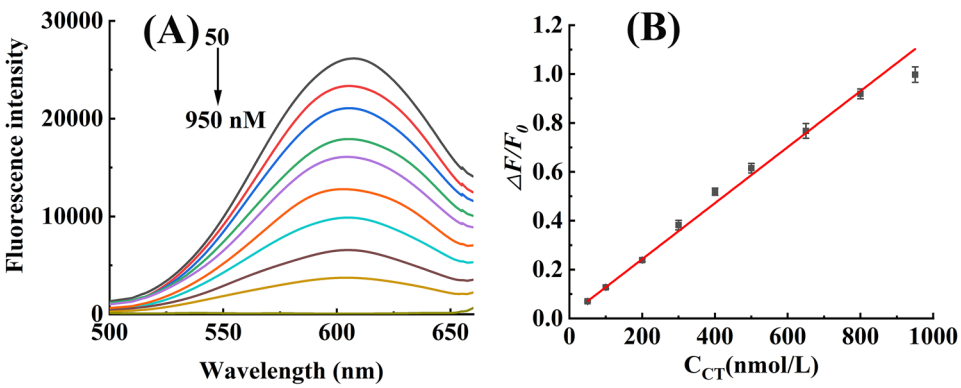

Fig. 5 Fluorescence emission spectra of hairpin DNA-CuNCs in the presence of different concentrations of *C. trachomatis* target DNA (from 50 to 950 nM) (**A**) Fluorescent emission spectra. (**B**) The linear relationship between the fluorescence intensity and *C. trachomatis* concentrations

Table 2 Comparison of the present work with other reported methods for detection of *C. trachomatis*

Methods	Detection principle	Linear range	LOD	Detection time	Particular conditions	Reference
Qualitative	Enzyme linked immunosorbent assay	-	-		With antibody	[26]
	PCR fluorescence probe method		-	4.5–5 h	With enzyme	[27]
	Fluorescent antibody technique		-	> 2 h	With antibody	[28–30]
	Multiplex thermostable recombinase polymerase amplification-lateral flow detection		-	15–20 min	With label	[31]
	Loop-mediated isothermal amplification-AuNPs-based colorimetric biosensing method		11.25 copies	< 1 h	With 6 primers	[32]
	The cobas 4800 CT/NG assay		320 ifu/mL	4–5 h	With isothermal DNA amplification	[33]
Quantitative	Multiple fluorescent quantitative PCR	10^9–10^2 copies/mL	1.0×10^2 copies/mL	-	With enzyme	[34]
	Multiplexed nanoplasmonic biosensor	10^3–10^8 cfu/mL	300 CFU/mL	-	With antibody	[35]
	Fluorescent biosensor by using flap endonuclease-assisted amplification	0–1 nM	6.7 pM	35 min	With enzyme	[36]
	Fluorescent biosensor based on hairpin DNA-CuCNs	50–950 nM	18.5 nM	5 min	Enzyme-free and label-free	This work

respectively. The above results proved the precision of the method constructed in this experiment has good accuracy.

Method Selectivity

To investigate the selectivity of the hairpin DNA-CuNCs toward *C. trachomatis* (CT), the effect of some probable microbial nucleic acid sequences (HPV, HSV-2, *Lactobacillus*, *Candida albicans*, *Treponema pallidum*, *Neisseria gonorrhoeae*, *Ureaplasma urealyticum*) was investigated under identical conditions. Figure 6 displayed the fluorescence response observed upon different sequences. Our research found that only addition of *C. trachomatis* caused a remarkable fluorescence signal changes, while other interference sequences almost had no influence on the fluorescence signal changes. This was owing to the high specificity of base complementary pairing, and the interference sequence failed to bind to the probe part of hairpin DNA, resulting in almost no change in fluorescence signal. Furthermore, the mixture of *C. trachomatis* and other interference sequences (The column on the far right) could cause a significant fluorescence signal changes, indicating that other interference sequences were unable to affect the detection of *C. trachomatis*. According to the above analysis, the fluorescent biosensor based on hairpin DNA-CuNCs possessed strong specificity for *C. trachomatis*.

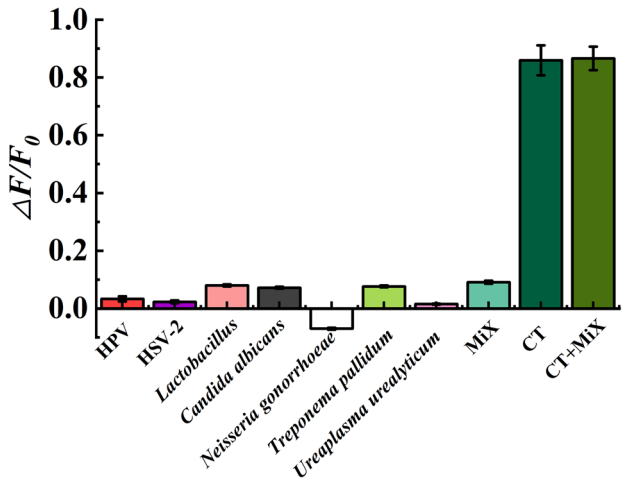

Fig. 6 Effect of interfering sequences on the fluorescence of the sensing system

Recovery Text

To evaluate the applicability of the proposed method in actual samples, different concentrations of *C. trachomatis* sequence were added to Hela cell lysates. The fluorescence intensity of each system was recorded by fluorescence spectrophotometer, and the concentration of *C. trachomatis* sequence was calculated according to the fluorescence intensity. All of the measurements were performed 6 times. The results were listed in Table 3, the recoveries for the complex samples with *C. trachomatis omp1* sequence (0.2 M, 0.4 M and 0.65 M) added were 102.25%, 101.83% and 104.04%, respectively. Moreover, relative standard deviation (RSD) for the recovery test was found to be below 5%. The results

Table 3 Determination results of target sequence of *C. trachomatis* in samples

Sample	Added(μM)	Detected(μM)	Recovery(%)	RSD
Hela cell lysates	0.20	0.20	102.25%	4.80%
	0.40	0.41	101.83%	3.26%
	0.65	0.68	104.04%	3.89%

demonstrated that the developed method provided a potential assay of *C. trachomatis* sequence in real sample.

Conclusions

In summary, we developed a simple, rapid, high sensitive and selective fluorescence biosensor based on hairpin DNA-CuNCs for *C. trachomatis* detection. In the present of *C. trachomatis* target DNA, the base complementary pair binding of the target DNA and hairpin DNA probe caused the opening of hairpin DNA, resulting in the significant reduction of the fluorescence intensity of hairpin DNA-CuNCs. Based on this strategy, a good liner relationship between the concentrations of *C. trachomatis* target DNA and fluorescence signals were obtained from 50 to 950 nM, and the LOD was 18.5 nM. Furthermore, this method showed good recoveries for the *C. trachomatis omp1* gene detection in the Hela cell lysates samples. Owing to these advantages, this hairpin DNA-CuNCs-based strategy provided a new thought for the early diagnosis and treatment of *C. trachomatis* with broad application prospects.

Supplementary Information The online version contains supplementary material available at https://doi.org/10.1007/s10895-022-02961-y.

Authors' Contributions Conceptualization and supervision: LC and HL; major contributor in writing the manuscript: LL and XZ; review and editing: QB, CL and ZL.

Funding This work was supported by the National Natural Science Fund of China (81903369), the Natural Science Foundation of Hunan Province (2020JJ4527, 2019JJ50491), the Scientific Research Fund of Hunan Provincial Education Department (20A438), the Fund of Hunan Key Laboratory (2019TP1027), and the Fund of University of South China Postgraduate Research Innovation Project (203YXC020).

Data Availability The data sets supporting the results of this article are included within the article and its additional files.

Code Availability Not applicable.

Declarations

Ethics Approval Not applicable.

Consent to Participate (Include Appropriate Statements) All authors acknowledge participation in this manuscript.

Consent for Publication (Include Appropriate Statements) All authors have read and agreed to the published version of the manuscript.

Conflicts of Interest The authors declare that they have no competing interests.

References

1. Gitsels A, Sanders N, Vanrompay D (2019) Chlamydial Infection From Outside to Inside. Front Microbiol 10:2329. https://doi.org/10.3389/fmicb.2019.02329
2. Wiesenfeld HC (2017) Screening for *Chlamydia trachomatis* Infections in Women. N Engl J Med 376:765–773. https://doi.org/10.1056/NEJMcp1412935
3. Dolat L, Valdivia RH (2019) A renewed tool kit to explore *Chlamydia pathogenesis*: from molecular genetics to new infection models. F1000Res 8:935–944. https://doi.org/10.12688/f1000research.18832.1.
4. Kunz TC, Götz R, Sauer M, Rudel T (2019) Detection of *Chlamydia* Developmental Forms and Secreted Effectors by Expansion Microscopy. Front Cell Infect Microbiol 9:276. https://doi.org/10.3389/fcimb.2019.00276
5. Briese T, Palacios G, Kokoris M, Jabado O, Liu Z, Renwick N, Kapoor V, Casas I, Pozo F, Limberger R, Perez-Brena P, Ju J, Lipkin WI (2005) Diagnostic system for rapid and sensitive differential detection of pathogens. Emerg Infect Dis 11:310–313. https://doi.org/10.3201/eid1102.040492
6. Mazraani R, Timms P, Hill PC, Suaalii-Sauni T, Niupulusu T, Temese SVA, Iosefa-Siitia L, Auvaa L, Tapelu SA, Motu MF, Righarts A, Walsh MS, Rombauts L, Allan JA, Horner P, Huston WM (2019) Evaluation of a PGP3 ELISA for surveillance of the burden of *Chlamydia* infection in women from Australia and Samoa. Pathog Dis 77:tz031. https://doi.org/10.1093/femspd/ftz031
7. Sood S, Mukherjee A, Bala M, Satpathy G, Mahajan N, Sharma A, Kapil A, Sharma VK, Pandey RM, Samantaray JC (2012) A pilot study for diagnosis of genital *Chlamydia trachomatis* infections by polymerase chain reaction among symptomatic Indian women. Indian J Dermatol Venereol Leprol 78:443–447. https://doi.org/10.4103/0378-6323.98074
8. Zhang Y, Cao L, Xu Z, Zhu P, Huang B, Li K, Xu Y, Zhang Z, Wu Y, Di B (2020) Evaluation of a multiplex PCR assay for detection of respiratory viruses and Mycoplasma pneumoniae in oropharyngeal swab samples from outpatients. J Clin Lab Anal 34:e23032. https://doi.org/10.1002/jcla.23032
9. van Dommelen L, Wolffs PF, van Tiel FH, Dukers N, Herngreen SB, Bruggeman CA, Hoebe CJ (2013) Influence of temperature, medium, and storage duration on *Chlamydia trachomatis* DNA detection by PCR. J Clin Microbiol 51:990–992. https://doi.org/10.1128/JCM.02631-12
10. Klint M, Löfdahl M, Ek C, Airell A, Berglund T, Herrmann B (2006) Lymphogranuloma venereum prevalence in Sweden among men who have sex with men and characterization of *Chlamydia trachomatis* ompA genotypes. J Clin Microbiol 44:4066–4071. https://doi.org/10.1128/JCM.00574-06
11. Black CM, Marrazzo J, Johnson RE, Hook EW 3rd, Jones RB, Green TA, Schachter J, Stamm WE, Bolan G, St Louis ME, Martin DH (2002) Head-to-head multicenter comparison of DNA probe and nucleic acid amplification tests for *Chlamydia trachomatis* infection in women performed with an improved reference standard. J Clin Microbiol 40:3757–3763. https://doi.org/10.1128/JCM.40.10.3757-3763.2002
12. Bryan ER, McLachlan RI, Rombauts L, Katz DJ, Yazdani A, Bogoevski K, Chang C, Giles ML, Carey AJ, Armitage CW, Trim

LK, McLaughlin EA, Beagley KW (2019) Detection of *chlamydia* infection within human testicular biopsies. Hum Reprod 34:1891–1898. https://doi.org/10.1093/humrep/dez169
13. Liu G, Shao Y, Peng J, Dai W, Liu L, Xu S, Wu F, Wu X (2013) Highly thymine-dependent formation of fluorescent copper nanoparticles templated by ss-DNA. Nanotechnology 24:345502. https://doi.org/10.1088/0957-4484/24/34/345502
14. Mao X, Liu S, Yang C, Liu F, Wang K, Chen G (2016) Colorimetric detection of hepatitis B virus (HBV) DNA based on DNA-templated copper nanoclusters. Anal Chim Acta 909:101–108. https://doi.org/10.1016/j.aca.2016.01.009
15. Peng XS, Chen SY, Ou LJ, Luo FW, Qin SW, Sun AM (2018) Hairpin loop-enhanced fluorescent copper nanoclusters and application in S1 nuclease detection. Analyst 143:415–419. https://doi.org/10.1039/c7an01725a
16. Wang Y, Cui H, Cao Z, Lau C, Lu J (2016) Additive and enhanced fluorescence effects of hairpin DNA template-based copper nanoparticles and their application for the detection of NAD^+. Talanta 154:574–580. https://doi.org/10.1016/j.talanta.2015.12.067
17. Zhang Y, Zhu Z, Teng X, Lai Y, Pu S, Pang P, Wang H, Yang C, Barrow CJ, Yang W (2019) Enzyme-free fluorescent detection of microcystin-LR using hairpin DNA-templated copper nanoclusters as signal indicator. Talanta 202:279–284. https://doi.org/10.1016/j.talanta.2019.05.013
18. Chen CA, Wang CC, Jong YJ, Wu SM (2015) Label-Free Fluorescent Copper Nanoclusters for Genotyping of Deletion and Duplication of Duchenne Muscular Dystrophy. Anal Chem 87:6228–6232. https://doi.org/10.1021/acs.analchem.5b00918
19. Mu J, Peng Y, Shi Z, Zhang D, Jia Q (2021) Copper nanocluster composites for analytical (bio)-sensing and imaging: a review. Mikrochim Acta. https://doi.org/10.1007/s00604-021-05011-9
20. Qing T, Qian C, Xiaojun B, Gang L, Juan Y (2021) Preparation of DNA Origami Belt and Effect of pH on Its Stability. Chinese J Anal Chem 49:743–751
21. Chai YL, Gao ZB, Li Z, He LL, Yu F, Yu SC, Wang J, Tian YM, Liu LE, Wang YL, Wu YJ (2020) A novel fluorescent nanoprobe that based on poly(thymine) single strand DNA-templated copper nanocluster for the detection of hydrogen peroxide. Spectrochim Acta A Mol Biomol Spectrosc 239:118546. https://doi.org/10.1016/j.saa.2020.118546
22. Zhang H, Lin Z, Su X (2015) Label-free detection of exonuclease III by sing dsDNA–templated copper nanoparticles as fluorescent probe. Talanta 131:59–63
23. Luo T, Zhang S, Wang Y, Wang M, Liao M, Kou X (2017) Glutathione-stabilized Cu nanocluster-based fluorescent probe for sensitive and selective detection of Hg^{2+} in water. Luminescence 32:1092–1099. https://doi.org/10.1002/bio.3296
24. Pang J, Lu Y, Gao X, He L, Sun J, Yang F, Liu Y (2020) Single-strand DNA-scaffolded copper nanoclusters for the determination of inorganic pyrophosphatase activity and screening of its inhibitor. Mikrochim Acta 187:672. https://doi.org/10.1007/s00604-020-04647-3
25. Hu Y, Wu Y, Chen T, Chu X, Yu R (2013) Double-strand DNA-templated synthesis of copper nanoclusters as novel fluorescence probe for label-free detection of biothiols. Anal Methods 5:3577–3581. https://doi.org/10.1039/C3AY40088C
26. van Ess EF, Ouburg S, Land JA, Morré SA (2018) Comparison of the Mikrogen multi-target ELISA with the Mikrogen recomLine immunoblot for the detection of Chlamydia trachomatis IgG antibodies in serum in infertile women. J Microbiol Methods 150:5–8. https://doi.org/10.1016/j.mimet.2018.05.006
27. Qinwan W, Qi Z (2018) Application of PCR with fluorescent probe to test for Chlamydia trachomatis, Neisseria gonorrhoeae and Ureaplasma urelyticum in secretion. Chin J Biologicals 31:307–310
28. Salari SH, Ward ME (1979) Early detection of Chlamydia-trachomatis using fluorescent DNA-binding dyes. J Clin Pathol 32:1155–1162
29. Bell TA, Kuo CC, Stamm WE, Tam MR, Stephens RS, Holmes KK, Grayston JT (1984) Direct fluorescent monoclonal antibody stain for rapid detection of infant Chlamydia trachomatis infections. Pediatrics 74:224–228
30. Grossgebauer K, Rolly H (1982) Fluorescent, DNA-binding dyes for rapid detection of Chlamydia trachomatis. Microsc Acta 86:1–11
31. Zhai J, Wang L, Qiao X, Zhao J, Wang X, He X (2021) Detection of Neisseria gonorrhoeae and Chlamydia trachomatis infections in pregnant women by multiplex recombinase polymerase amplification. PLoS ONE 16:e0251119. https://doi.org/10.1371/journal.pone.0251119
32. Somboonna N, Choopara I, Arunrut N, Sukhonpan K, Sayasathid J, Dean D, Kiatpathomchai W (2018) Rapid and sensitive detection of Chlamydia trachomatis sexually transmitted infections in resource-constrained settings in Thailand at the point-of-care. PLoS Negl Trop Dis 12:e0006900. https://doi.org/10.1371/journal.pntd.0006900
33. Niekerk JM, van der Veer BMJW, Hoebe CJPA, van de Bovenkamp J, van Herk C, van Loo IHM, van Alphen LB, Wolffs PFG (2021) Despite Excellent Test Characteristics of the cobas 4800 CT/NG Assay, Detection of Oropharyngeal Chlamydia trachomatis and Neisseria gonorrhoeae Remains Challenging. J Clin Microbiol 59:e02137-e2220. https://doi.org/10.1128/JCM.02137-20
34. Pengfei C, Jingfeng T, Hongxia C, Liu Xu, Yefu W (2014) Development and clinical application of multiple fluorescent quantitative PCR methods for simultaneous detection of Neisseria agonorrhoeae, Chlamydia trachomatis and Ureaplasma parvum. Chinese Journal of Biologicals 27:109–114
35. Soler M, Belushkin A, Cavallini A, Kebbi-Beghdadi C, Greub G, Altug H (2017) Multiplexed nanoplasmonic biosensor for one-step simultaneous detection of Chlamydia trachomatis and Neisseria gonorrhoeae in urine. Biosens Bioelectron 94:560–567. https://doi.org/10.1016/j.bios.2017.03.047
36. Lee CY, Jang H, Kim H, Jung Y, Park KS, Park HG (2019) Sensitive detection of DNA from Chlamydia trachomatis by using flap endonuclease-assisted amplification and graphene oxide-based fluorescence signaling. Mikrochim Acta 186:330. https://doi.org/10.1007/s00604-019-3453-2